Chemistry & Biology, Vol. 9, 403–415, April, 2002, ©2002 Elsevier Science Ltd. All rights reserved. PII S1074-5521(02)00121-7

Oxidative Charge Transport through DNA in Nucleosome Core Particles

Megan E. Núñez, Katherine T. Noyes, and Jacqueline K. Barton[1]
Division of Chemistry and Chemical Engineering,
California Institute of Technology
Pasadena, California 91125

Summary

Eukaryotic DNA is packaged into nucleosomes, made up of 146 bp of DNA wrapped around a core of histone proteins. We used photoexcited rhodium intercalators to explore DNA charge transport within these assemblies. Although histone proteins inhibit intercalation of the rhodium complex within the core particle, they do not prevent 5′-GG-3′ oxidation, the signature of oxidative charge transport through DNA. Moreover, using rhodium intercalators tethered to the 5′ terminus of the DNA, we found that guanine bases within the nucleosome can be oxidized from a distance of 24 bp. Histone binding did not affect the pattern and extent of this oxidation. Therefore, although the structure of the nucleosome core particle generally protects DNA from damage by solution-borne molecules, packaging within the nucleosome does not protect DNA from charge transfer damage through the base pair stack.

Introduction

The question of whether double-helical DNA provides an effective conduit for charge transport has fascinated scientists since its structure was first elucidated. The idea that the stacking of the π orbitals on the aromatic, heterocyclic base pairs not only confers stability to the polymeric assembly but also may provide a basis for charge transport has been examined by biologists, physicists, and chemists for years [1–3]. The variety of studies carried out now show that although the rates and efficiencies of electron transfer through DNA vary considerably depending upon the system employed, charges can indeed migrate through DNA. One sensitive parameter governing this charge transport is stacking of the donor and acceptor within the DNA base pair stack. When there is effective orbital overlap between the DNA π stack and the reactants, fast, efficient charge transport is possible.

Not only can electron transfer mediated by the DNA be facile, but the π stack can serve as a reactant in the electron transfer process. Radicals can migrate through the helix to react at a remote site from an oxidant bound to the DNA. Oxidative damage to DNA *from a distance* was first demonstrated in an assembly containing a tethered photooxidizing rhodium intercalator (Figure 1A) spatially separated from the sites of oxidation [4]. The 5′ guanine of 5′-GG-3′ sites is selectively oxidized based on its redox potential and stacking characteristics [5–7]. As for electron transfer kinetics monitored spectroscopically, oxidative damage to DNA mediated by the base pair stack shows a shallow dependence on distance, but an exquisite sensitivity to stacking [8, 9]. This ability to mediate long-range charge transport is a characteristic of the DNA duplex, not the oxidant, since a variety of different intercalators have been shown to oxidize guanine doublets from a distance [10–19].

In our efforts to determine whether DNA charge transport is a biologically relevant phenomenon, we have determined that charge transport to damage 5′-GG-3′ sites can occur over tens of base pairs on oligonucleotides and restriction fragments to effect DNA damage [9, 18]. However, DNA inside of cells is intimately associated with a variety of proteins that serve to regulate replication and transcription as well as to repair and package the DNA itself [20].

In studies of long-range guanine oxidation on oligonucleotide assemblies, it was demonstrated first that the binding of a variety of proteins to DNA can sensitively modulate charge transport through the helix, depending on their effects on the stacking of the DNA base pairs. M.HhaI is a DNA methylase which, in binding its target site, flips out the cytosine for methylation, inserts a glutamine side chain, and thus stabilizes a "gap" in the DNA π stack [21]. As a result of the gap, M.HhaI inhibits oxidative damage to DNA past its binding site. However, a mutant M.HhaI that inserts a tryptophan into the gap created by base flipping does not inhibit charge transport on binding to DNA, probably because the flat, aromatic tryptophan side chain of the mutant protein restores the π-stacked array needed for charge transport through the helix. TATA binding protein (TBP) generates two approximately 90° kinks on either end of its recognition site upon binding to DNA, and consistent with the requirement of stacking for effective charge transport, binding of TBP seriously disrupts π stacking and long-range charge transport [22]. PvuII restriction endonuclease and *Antennapedia* homeodomain protein do not significantly distort the π stack upon binding to DNA, and as a consequence do not inhibit long-range charge transport [22]. To the contrary, the binding of either protein somewhat increases long-range guanine oxidation, presumably because the proteins facilitate charge transport by restricting the dynamic motions of the DNA bases and stiffening the DNA helix.

The fundamental unit of DNA packing inside eukaryotic cells is the nucleosome core particle (NCP), in which approximately 150 base pairs of DNA are bound around an octamer of histone proteins [23]. These particles are then assembled into higher-order structures, stabilized by other histone- and non-histone-proteins, in order to further compact the DNA so as to fit into the nucleus. In addition to packaging DNA, the histone proteins may serve both regulatory and protective functions. Given the ubiquity of the nucleosome, the potential involvement of the histone octamer in modulating charge migration through DNA is therefore of significant interest.

The structure of an NCP has been determined for a

[1]Correspondence: jkbarton@caltech.edu

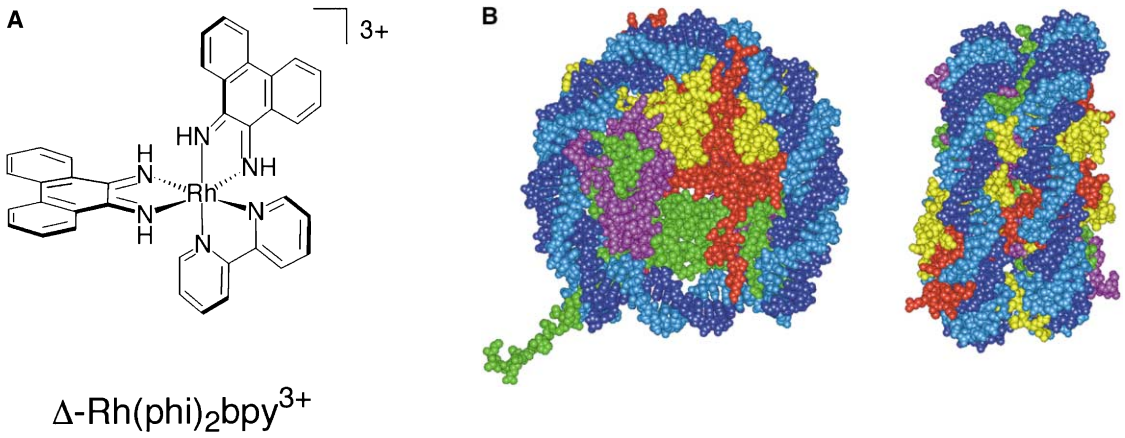

Figure 1. Structures of the Molecules Used in This Study

(A) The rhodium complex $Rh(phi)_2DMB^{3+}$ (phi = phenanthrene quinone diimine; DMB = 4,4′-dimethyl- 2,2′-bipyridine), which binds avidly to DNA by intercalation of one of its phi ligands [58]. This complex can also be functionalized on the bipyridine ligand so as to covalently attach it to the 5′ terminus of the DNA.

(B) The nucleosome core particle. A length of 146 bp of DNA (blue and cyan) is wrapped one-and-two-thirds times around an octamer of histone proteins [24, 28]. In order to wrap around the histones, the DNA is heterogeneously bent and overwound. The octamer is composed of two each of histones 2A (red), 2B (yellow), 3 (green), and 4 (purple), which bind nonspecifically to the DNA by a variety of electrostatic, hydrogen bonding, and nonpolar interactions. (The picture was adapted from Protein Data Bank coordinates 1aoi, reference [24].)

histone octamer and a 146 bp palindromic DNA sequence [24]. In this structure, the DNA is highly bent as it wraps 1.65 times around the outside of the histone octamer and forms a "superhelix" with a diameter around 42 Å (Figure 1B). The overall twist of the base pairs is 10.2 bp per turn, in contrast to the 10.5 bp per turn observed in solution, although there is considerable variability between different positions on the core particle. The combination of the base pair twist and the superhelix winding gives an overall *over*winding of nucleosomal DNA compared to DNA in solution. The bending and relative mobility of the DNA are also heterogeneous in response to local histone-DNA interactions. Some regions of the DNA are highly kinked, whereas others are quite straight. Exposed sections of the DNA are flexible and mobile, and histone-bound sections of the DNA are dynamically restricted.

The fact that DNA-histone contacts are nonspecific does not imply that all DNA sequences bind equally well to form a core particle. Clearly, those sequences that are inherently more flexible or that contain correctly phased bends will bind the histone octamer more readily than other sequences [25–27]. It has been observed that A-T base pairs are preferred where the minor groove faces inwards toward the histone core and that G-C pairs are preferred where the major groove faces inwards because those base pair combinations bend more readily in those directions. As a result, placement of certain sequences can impart a rotational orientation upon the NCP. In the case of the DNA sequence for which the NCP structure was solved, the 146 bp sequence contains 12 known nucleosome phasing regions, which predispose it to form a single, stable conformation with the histone octamer [28].

Because the histone ocamer must accommodate a range of different DNA sequences, the interactions between the protein core and the DNA are generally nonspecific and largely electrostatic [23, 24]. Therefore, the surface of the octamer has an overall positive charge, in contrast to the negative charge of the DNA polyanion. In addition to hydrogen bonds between arginine side chains in the minor groove and DNA backbone phosphates, other stabilizing interactions include hydrogen bonds between phosphates and main-chain amide nitrogen atoms as well as interactions between phosphates and helix dipoles [24]. Extensive nonpolar contacts between the protein and deoxyribose groups as well as hydrogen bonds and salt links between phosphates and other protein side chains also help to stabilize the protein-DNA interaction. Although some side chains do protrude into both grooves, they make few contacts with bases.

Here we examine guanine oxidation by rhodium intercalators in NCPs to determine the effect of DNA packaging on long-range charge transport through the base pair stack. Given that the DNA in the core particle is overwound, bent, and in some places dynamically restricted, DNA binding to histones in this structure might serve to protect nucleosomal DNA from long-range oxidative damage. Alternatively, such packaging might decrease the flexibility of the DNA and provide a unique and isolated medium to facilitate charge transport through the DNA base pair stack.

Results

Sequence of the Nucleosomal DNA within the Core Particle

A radioactively labeled 146-mer oligonucleotide, duplex **1**, was used to examine oxidative damage to DNA within the NCP (Figure 2). This sequence was selected because it forms a stable NCP that has a single rotational and

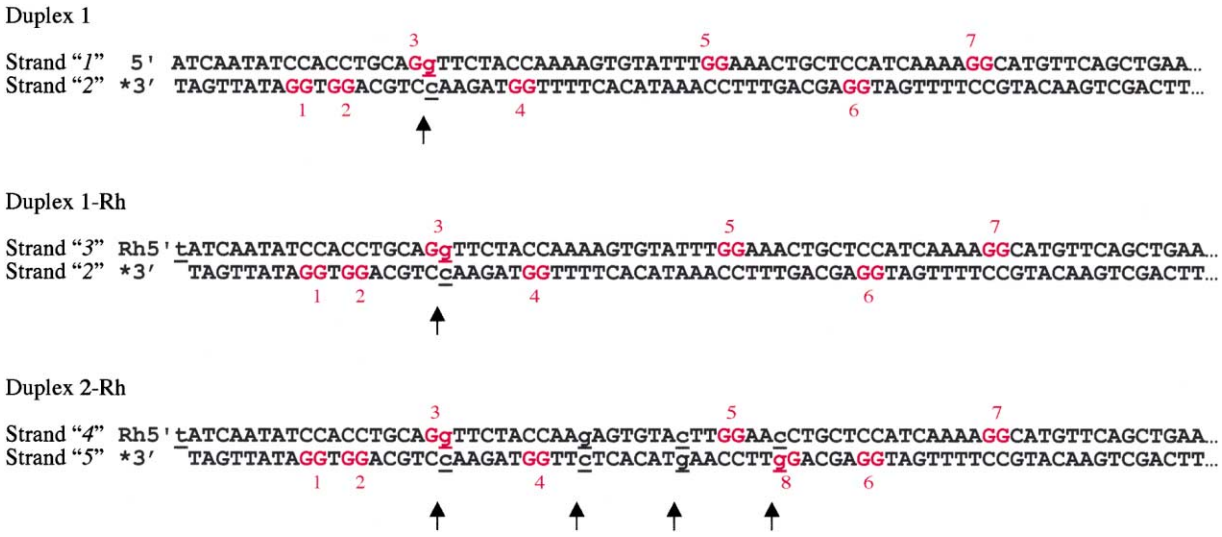

Figure 2. Sequences of Half of Palindromic DNA Oligonucleotide Duplexes

An asterisk indicates a radioactive label. Bases that were changed from the original sequence of Luger et al. are indicated by lowercase/underlining and dark-gray arrows. Red numbers correspond to the 5′-GG-3′ sequences; corresponding 5′-GG-3′ sequences on the other half of the palindrome are numbered identically.

translational setting and whose structure with both recombinant frog and purified chicken histone proteins has been solved crystallographically [24, 28]. Significantly, the DNA sequence of duplex **1** is palindromic, which means that both strands are identical when read from the 5′ to the 3′ direction. Additionally, it means that both halves of the sequence, from the termini to the center, are identical. In the crystal the 146-mer binds to the C2-symmetric histone octamer with the center of the palindromic sequence almost aligned with the rotational symmetry axis of the octamer. Because this alignment is off by only approximately half of a base pair at the C2 symmetry axis, for the purposes of this study we assume that the two halves of the DNA structure are also identical. Structures shown here display only one half (73 bp) of the sequence, corresponding to ~0.8 turns around the NCP from the DNA terminus to the center.

In designing these experiments, only one base pair was changed from the sequence used previously [24] in each half of duplex **1** in order to add a 5′-GG-3′ site by which to monitor long-range charge transport to oxidize DNA bases (Figure 2). As a result, the sequence contains seven 5′-GG-3′ sequences in each half of the palindrome that (in the absence of guanine triplets) are expected to be the most easily oxidized sites on the duplex. These 5′-GG-3′ sites are numbered GG1 through GG7 from the terminus of the sequence to the center. Because of the palindromic nature of the sequence, the full 146 bp duplex actually contains 14 5′-GG-3′ sites, seven on each identical strand. When viewed on a denaturing polyacrylamide gel, all seven 5′-GG-3′ sites can potentially be seen in the order GG1, GG2, GG4, GG6, (center), GG7, GG5, GG3 from the radiolabeled 3′ terminus at the bottom of the gel to the 5′ terminus at the top.

Confirmation of the Structure of the Nucleosome Core Particle by DNase I Footprinting

Histone octamers can be exchanged from one piece of DNA to another by incubation with high concentrations of salt (i.e., 1 M NaCl) followed by dilution or dialysis [29]. Salt exchange of histone octamers from purified chicken DNA to duplex **1** resulted in the formation of a single species with a larger molecular weight than the parent 146-mer as determined by nondenaturing gel electrophoresis (not shown). This larger species was isolated from the gel. DNase I footprinting was used to confirm that the histone proteins were bound specifically to the 146-mer to form an NCP with the same structure as that elucidated crytallographically [24, 28]. Samples lacking histone proteins are cleaved more quickly and at a lower concentration of DNase I than are samples with histones (Figure 3A). This slower cleavage is one indication that the 146-mer is bound to the histones and thus protected by them from cleavage. Slower cleavage by DNase I could be due to competition for DNase I by contaminating chicken DNA; however, studies with the same concentrations of NCPs that were *not* exchanged onto the target radiolabeled DNA indicate that the protective effect of the histone proteins is largely due to their binding to the DNA. More interestingly, the pattern of DNase I cleavage on the histone bound 146-mer displays regions of periodic protection from and accessibility to DNase I (Figure 3A). This pattern is distinct from the more random pattern of enzyme cleavage on the bare 146-mer. The distinct pattern of periodic cleavage is characteristic of DNA in NCPs and not of DNA with randomly bound histones. Furthermore, the pattern indicates uniform phasing of the DNA relative to the protein. This uniform phasing is expected in light of the fact that this sequence contains 12 phased positioning sequences [28]. On longer pieces of DNA, it is

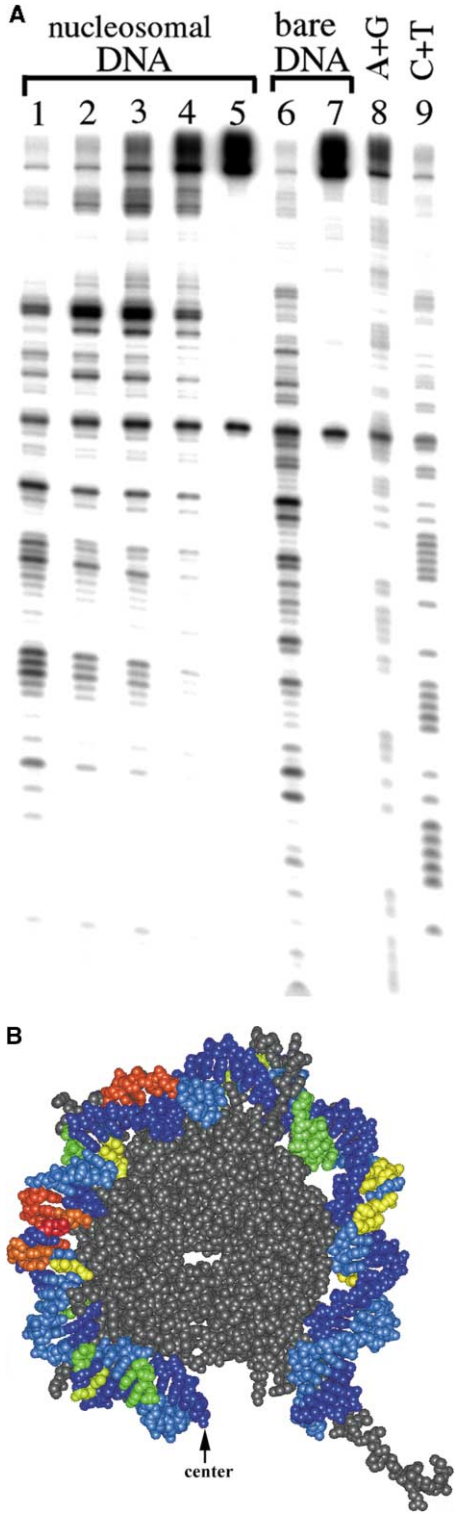

Figure 3. DNase I Digestion of Duplex **1** with and without Bound Histone Proteins

(A) Lanes 1–5 have bound histone proteins, whereas lanes 6 and 7 do not; lanes 8 and 9 are Maxam-Gilbert purine- and pyrimidine-specific sequencing lanes, respectively. DNase I was added to each sample in the following amounts: lane 1, 2.5 U; lane 2, 0.5 U; lane 3, 0.25 U; lane 4, 0.05 U; lane 5, no enzyme; lane 6, 0.05 U; lane 7, no enzyme. The band present at the center of the gel in all lanes is due to incomplete ligation to form the 146-mer. Details of the digestion are explained in the Experimental Procedures. Note that bare DNA is cut more readily than histone bound DNA and that the pattern of cleavage by the DNase I enzyme in the presence of bound histone proteins is distinct from the pattern of cleavage in the absence of proteins.

(B) Cleavage of histone bound duplex **1** superimposed upon the crystal structure of the same sequence in a nucleosome core particle [24]. The histone octamer is colored gray; one-half of the 146-mer palindromic DNA is shown in a range of colors. Blue and cyan regions were not cut by the enzyme in either the presence or absence of histones; yellow regions were cut by the enzyme fairly equally in the presence or absence of histones. Red and orange regions were *hyper*sensitive to DNase I when duplex **1** was bound to the histones; green regions were *hypo*sensitive to DNase I. Estimates of cleavage intensities are approximate and are based upon samples in which the total amount of cleavage was roughly equal. Because the enzyme cleaves bare DNA much more readily than it cleaves protein bound DNA, histone bound samples were incubated for a longer time period and with more DNase I enzyme than bare DNA samples. The 2-fold rotational symmetry axis through the center of the NCP is indicated by the arrow. (The picture was adapted from Protein Data Bank coordinates 1aoi, reference [24].)

possible to have several species with the same rotational phasing but different translational orientations. However, because this radiolabeled DNA is only 146 bp (the minimum length of DNA required to bind entirely around a histone octamer), it is reasonable to expect one predominant form with the 146-mer bound (relatively) symmetrically to the histones to form core particles. The presence of a single predominant form is also consistent with the results of the gel shift assay.

The pattern of DNase I cleavage can also be used to determine where the minor groove faces outward into the solution and becomes accessible to the enzyme and where the minor groove faces inward toward the histone protein and is protected from the enzyme [30]. These cleavage patterns can then be mapped to the DNA in the crystal structure to establish whether the two views of the histone bound 146-mer DNA agree (Figure 3B). Regions of duplex **1** that are *hyper*sensitive to DNase I correspond to places where the minor groove bends outward into the solution, whereas regions of duplex **1** that are *hypo*sensitive to DNase I frequently correspond to places where the minor groove faces inward toward the histone octamer or where histone tails or side chains bind in the major groove. Interestingly, the DNase I cleavage in some regions of the sequence is unchanged, indicating that the accessibility or reactivity of some stretches of the DNA sequence is not affected by the binding to the histone proteins. Although the DNase I footprinting alone does not provide a clear picture of the core particle, it is fairly consistent with that provided by the crystal structure. This structural information is very useful because it not only tells us that our DNA is bound in an NCP but it potentially allows us to examine the accessibility of particular reactive sites (*vide infra*).

The structures of duplex **1-Rh** and **2-Rh** containing tethered rhodium intercalators could not be examined similarly via DNase I footprinting because the rhodium-tethered oligonucleotides cannot be extracted with phenol and chloroform. However, gel shift experiments indicate that a single histone bound species is formed by nucleosome exchange (not shown).

Binding and Oxidation by Noncovalent $Rh(phi)_2DMB^{3+}$ on a 146-mer

$Rh(phi)_2DMB^{3+}$ (phi = phenanthrene quinone diimine; DMB = 4,4′-dimethyl-2,2′-bipyridine) binds avidly to DNA by intercalation and reacts with DNA according to two distinct mechanisms. With irradiation at 313 nm, phi complexes of rhodium cleave the sugar-phosphate backbone at their intercalation site, allowing determination of where they are bound [31, 32]. These complexes bind DNA with very little sequence preference, and thus photoirradiation at 313 nm yields a broad distribution of cleavage sites. The products of this reaction, which are consistent with abstraction of the 3′ hydrogen by the metal complex, lead to strand breaks without further treatment of the DNA.

In contrast, when irradiated at 365 nm, the rhodium complexes preferentially oxidize the 5′ guanine of 5′-GG-3′ sites [4]. When spatially separated from the 5′-GG-3′ sites, the rhodium complexes can oxidize guanine bases by a long-range reaction that is mediated by the DNA base stack [4, 8, 9]. The mechanism of charge migration through the base pair stack is being explored currently, and the long-range reaction probably involves charge hopping through the stack [1, 15, 17]. The oxidized guanine base is ultimately trapped as a permanent lesion by reaction of the neutral guanine radical with water and oxygen. The oxidized products include not only 8-oxo-7,8-dihydroguanine [4], but also other lesions, probably imidazolone and oxazolone derivatives [33]. The various lesions are converted to direct strand breaks upon incubation of the DNA with hot aqueous piperidine or upon treatment with the enzyme formamidopyrimidine DNA glycosylase (Fapy glycosylase). Because treatment of these rhodium-induced photoproducts with either piperidine or Fapy glycosylase generates a similar pattern of strand breaks in comparable yields ([34]; our unpublished data), we revealed rhodium-induced photoproducts by piperidine incubation exclusively in these experiments.

Under certain reaction conditions the distinction between these two reactions is not always sharp [31]. Treatment of samples that have been photocleaved by rhodium at 313 nm with hot aqueous piperidine reveals some photooxidation at 5′-GG-3′ sites, and at high rhodium concentrations (>10 μM), photoexcitation at 365 nm leads to nonspecific DNA direct strand breaks as well as guanine base oxidation. This overlap of reactivity depends in part upon the efficiency of reactions at high concentrations and in part upon the fact that the light used for irradiation is dispersed over a range of wavelengths, including the excitation wavelengths for both reactions.

Photoirradiation can also lead to DNA-protein crosslinks, either as a direct result of photoexcitation of the DNA or protein by the light source or as a result of an interaction between a base or sugar radical on the DNA (generated by the rhodium photoreactions) with the histone proteins. The former reaction does not occur with irradiation at 313 or 365 nm because neither DNA nor histones absorb light at these wavelengths. However, histone-guanine crosslinking has been observed previously to occur after long-range oxidation of guanine bases by ruthenium polypyridyl complexes [34]. In this case, a substantial fraction of the DNA becomes covalently crosslinked to the histone proteins after photoirradiation with rhodium complexes. DNA-protein crosslinking is not surprising given the close proximity of the histone proteins to the DNA on which a radical intermediate is being formed; in the absence of protein, these radical intermediates are trapped by water or oxygen to form other oxidized base lesions [33]. In order to determine the location at which the radical is trapped, we treated all samples with proteinase K and hot aqueous piperidine after photoirradiation to break any DNA-protein crosslinks that were formed and reveal the location of the crosslinks. The locations of these cross-links were then visualized by denaturing gel electrophoresis as direct strand breaks. Although this method does not allow us to distinguish between oxidized guanine base lesions and crosslinked guanine sites, we can determine where the electronic "hole" on the DNA base stack was trapped, the primary question of interest.

Duplex **1**, both with and without bound histones, was incubated with 10 μM $Rh(phi)_2DMB^{3+}$, and the mixture was irradiated at 313 nm to determine sites of direct strand cleavage where the metal complex binds. In the absence of histone proteins, the rhodium complex binds and cleaves throughout the oligonucleotide duplex **1** in a nonspecific fashion, as evident upon photoirradiation at both 313 nm and 365 nm (Figure 4). This pattern of DNA damage is consistent with the fact that its concentration exceeds its nonspecific binding constant and the fact that the rhodium complex is present at high loading on the DNA.

When irradiated at 313 nm with the 146-mer oligonucleotide duplex **1** bound to histones as an NCP, the rhodium complex cleaves the DNA much less extensively (Figure 4), analogously to the way in which DNase I cleaves these same NCPs. What is especially interesting, however, is the *pattern* of direct DNA photocleavage. The distribution of rhodium photocleavage is not nonspecific, nor does it demonstrate a sequence specificity characteristic of $Rh(phi)_2DMB^{3+}$ at lower concentrations [31, 32]. The photocleavage does not show a periodic pattern of protection and exposure similar to cleavage by DNase I, hydroxyl radical, or micrococcal nuclease on NCPs. Instead, cleavage is observed exclusively at the 5′ guanine of 5′-GG-3′ sites (and at sites of direct photodynamic damage that are independent of rhodium). The damage pattern is the same, irrespective of irradiation at 313 nm or 365 nm.

To establish that the unusual patterns of cleavage were not due to rhodium concentration effects, we examined direct photocleavage and base oxidation in the same system by different concentrations of $Rh(phi)_2DMB^{3+}$ between 10 μM and 100 nM (Figure 5). On duplex **1** in the absence of histone proteins, the distribution of rhodium-induced DNA damage is fully consistent with previous studies [4, 31, 32]. At a concentration of 10 μM, the rhodium complex binds and photocleaves bare DNA nonspecifically at both 313 nm and 365 nm because the rhodium complex is present at a very high loading on the DNA. At 1 μM and lower concentrations, a weak sequence specificity in binding emerges (lanes 13–17). At 1 μM rhodium concentration, nonspecific cleavage at 365 nm is not evident, and charge transport damage

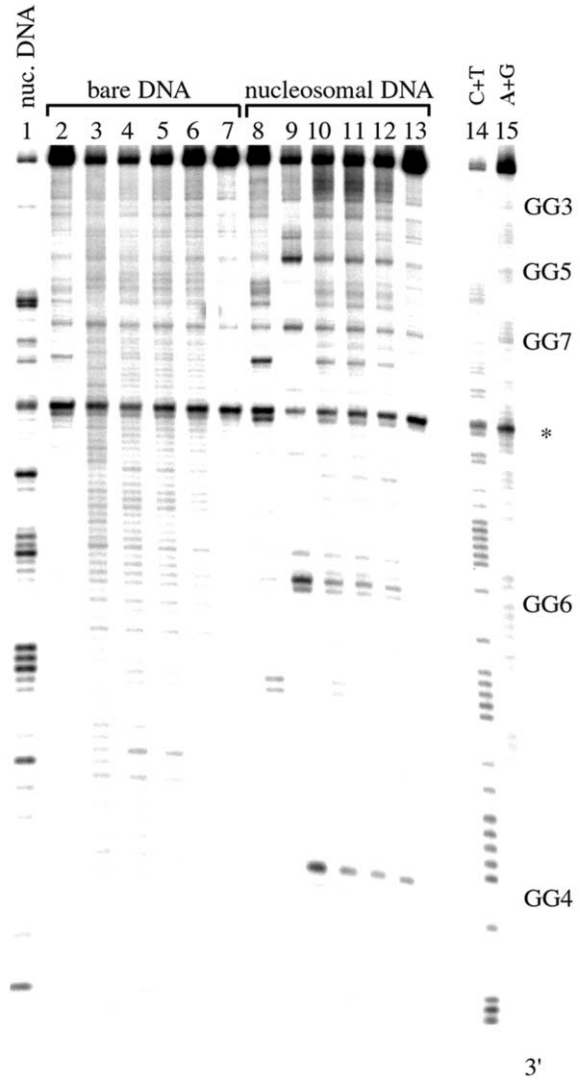

Figure 4. Direct Strand Scission and Base Oxidation by $Rh(phi)_2DMB^{3+}$ on Duplex **1** with and without Histone Proteins

DNA samples shown in lanes 1 and 8–13 are bound to histone proteins as nucleosome core particles; DNA samples in lanes 2–7 are bare DNA without histone proteins. Lane 1 is sequence 1 bound to histone proteins as a nucleosome core particle and digested with 2.5 U of DNase I for 5 min. Samples were photoirradiated with 10 μM noncovalent $Rh(phi)_2DMB^{3+}$ unless otherwise indicated, and all samples were treated with 10% piperidine for 30 min at 90°C after irradiation. Conditions for other lanes were as follows: lane 2, 10 min at 313 nm without rhodium complex; lane 3, 30 min at 365 nm; lane 4, 10 min at 313 nm; lane 5, 5 min at 313 nm; lane 6, 2 min at 313 nm; lane 7, no irradiation; lane 8, 30 min at 313 nm with no rhodium; lane 9, 90 min at 313 nm; lane 10, 30 min at 313 nm; lane 11, 20 min at 313 nm; lane 12, 10 min at 313 nm; and lane 13, no irradiation. Lanes 14 and 15 are Maxam-Gilbert pyrimidine-specific and purine-specific sequencing lanes, respectively. The band present at the center of the gel in all lanes and indicated by an asterisk is due to incomplete ligation to form the 146-mer.

is localized to 5′-GG-3′ sites (lane 20). However, in an NCP, the pattern of rhodium binding and direct strand scission at 313 nm on duplex **1** is distinctly different from that on bare DNA. Damage at both wavelengths is localized to the 5′ guanine of 5′-GG-3′ sites, which is the signature of charge transport damage through the DNA base pair stack.

Binding and Oxidation by $Rh(phi)_2bpy^{3+}$ Tethered to the 5′ Termini of the 146-mer

To determine the distances over which charges can migrate in nucleosomal DNA between 5′-GG-3′ sites and intercalating oxidants whose positions are known, we constructed duplex **1-Rh** with the same DNA sequence as duplex **1**, with a $Rh(phi)_2bpy'^{3+}$ complex covalently attached to each 5′ end (Figure 2). We have previously demonstrated that this complex is constrained by its diaminononane linker to intercalate 2 or 3 base pairs from the end of a DNA oligonucleotide duplex, from whence it can oxidize 5′-GG-3′ sites over approximately 200 Å [4, 9]. This radioactively labeled 146 bp oligonucleotide duplex **1-Rh**, modified with a tethered rhodium, was exchanged with histone octamers according to the same method as that in duplex **1**. Although the solubility of the resultant rhodium-tethered oligonucleotide precludes DNase I footprinting analysis, the behavior of this duplex by gel shift analysis is the same as that in duplex **1**. Given that the DNA sequence is identical to that of duplex **1** and the rhodium complexes are covalently attached to the termini, the structure of the nucleosome formed with duplex **1-Rh** is likely to be equivalent to that formed with duplex **1**.

Duplex **1-Rh** with or without bound histone proteins was photoirradiated at 313 nm and 365 nm (Figure 6, 7). In the *absence* of histone proteins, only oxidative base damage can be observed after irradiation at 313 nm (Figure 7). Strand scission at the intercalation site cannot be observed because the two symmetric termini of the 146-mer where we expect intercalation to occur are lost from the bottom of the gel and compressed near the top. Significantly, however, no other direct cleavage is observed, indicating that the metal complex is not binding to some other location in the sequence. With irradiation at both 365 nm and 313 nm and treatment with hot aqueous piperidine, oxidation is observed at GG1, GG2, GG3, and GG4, located 8, 11, 16, and 24 bp away from the closest intercalated metal complex if one assumes an intercalation site 3 bp in from its site of covalent attachment. The oxidation occurs selectively at the 5′ guanine of these 5′-GG-3′ sites. No significant oxidation is observed at the other guanine doublets positioned farther from the rhodium intercalation site, i.e., at GG5, GG6, and GG7. Importantly, in the presence of bound histone proteins, the pattern of damage with irradiation at both wavelengths is identical to the pattern of damage in the absence of bound histone proteins. This observation indicates that wrapping the 146-mer around a histone octamer to form an NCP does not change the rhodium intercalation into this sequence nor the long-range charge transport through it (Figure 6).

In this 146 bp sequence, no guanine oxidation is observed at guanine doublets GG5, GG6, and GG7, located 38, 48, and 56 bp away from the rhodium intercalator, even in the absence of bound protein. The absence of charge transport to oxidize guanine doublets over this distance contrasts with earlier observations with oligonucleotide duplexes [9, 15]. Because we had previously

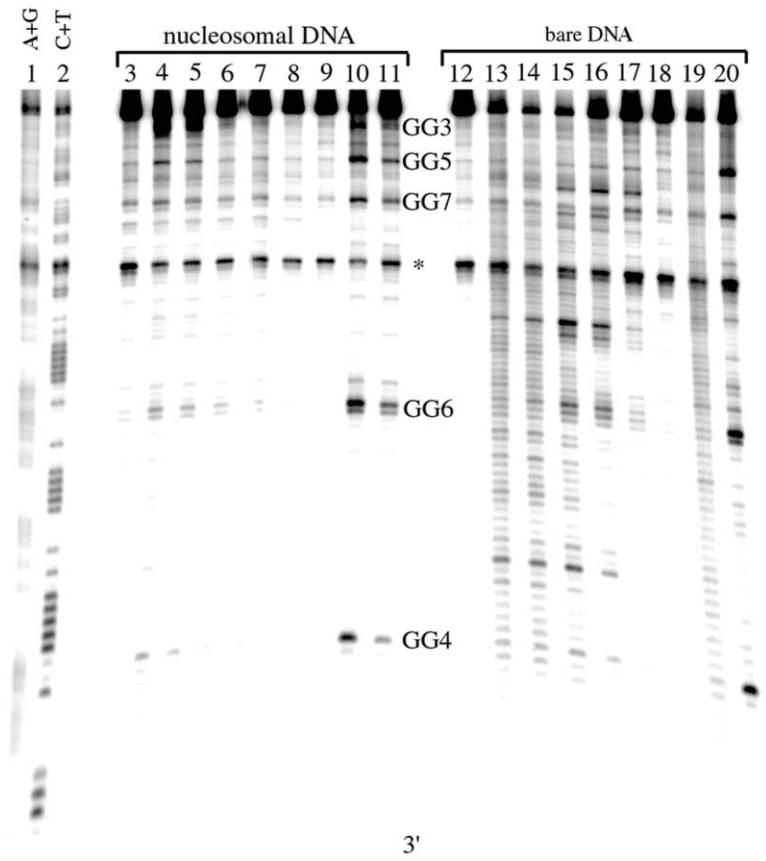

Figure 5. Direct Strand Scission and Base Oxidation Performed with Varying Concentrations of $Rh(phi)_2DMB^{3+}$ on Duplex **1** with and without Histone Proteins

DNA samples shown in lanes 3–11 are bound to histones as nucleosome core particles. DNA samples in lanes 12–20 are bare DNA without histone proteins. Lanes 1 and 2 are Maxam-Gilbert purine-specific and pyrimidine-specific sequencing lanes, respectively. Conditions for other lanes were as follows: lane 3, 10 μM rhodium, no photoirradiation; lane 4, 10 μM rhodium, 20 min at 313 nm; lane 5, 5 μM rhodium, 20 min at 313 nm; lane 6, 1 μM rhodium, 20 min at 313 nm; lane 7, 500 nM rhodium, 20 min at 313 nm; lane 8, 100 nM rhodium, 20 min at 313 nm; lane 9, no rhodium, 20 min at 313 nm; lane 10, 10 μM rhodium, 90 min at 365 nm; lane 11, 1 μM rhodium, 90 min at 365 nm; lane 12, 10 μM rhodium, no photoirradiation; lane 13, 10 μM rhodium, 10 min at 313 nm; lane 14, 5 μM rhodium, 10 min at 313 nm; lane 15, 1 μM rhodium, 10 min at 313 nm; lane 16, 500 nM rhodium, 10 min at 313 nm; lane 17, 100 nM rhodium, 10 min at 313 nm; lane 18, no rhodium, 10 min at 313 nm; lane 19, 10 μM rhodium, 30 min at 365 nm; and lane 20, 1 μM rhodium, 30 min at 365 nm. All samples were treated with 10% piperidine for 30 min at 90°C after photoirradiation. Indicated by an asterisk, the band at the center of the gel is due to incomplete ligation to form the 146-mer. 5′-GG-3′ sites are indicated by numbers corresponding to those in Figure 2.

observed an increase in long-range oxidative damage with increased temperature, we examined the guanine oxidation on duplex **1-Rh** in the presence and absence of histone proteins at various temperatures between 5°C and 35°C (Figure 8). However, in this case, variations in temperature do not change the increase in the yield of long-range oxidation, nor do they change the patterns of guanine oxidation on duplex **1-Rh**.

Subtle, temperature-independent differences in the pattern of guanine oxidation were caused by the binding of histone proteins in some experiments and can be seen here (Figure 8). Oxidation at the GG1 site is slightly increased, whereas oxidation at the GG4 site is slightly diminished in the presence as opposed to the absence of bound histones, but the changes in oxidation are very small. In general, the pattern of oxidation is relatively unchanged by DNA binding to histone proteins as an NCP.

Small changes in the DNA sequence were made to reduce its kinks and/or ability to bend in the absence of protein and to thereby increase the very long-range guanine oxidation (>30 bp). Duplex **2-Rh**, in which three AT base pairs in A-tract sequences were changed to GC base pairs in each half of the palindromic sequence, was constructed (Figure 2). This base pair change also introduced a new 5′-GG-3′ site into the sequence. Despite the changes in the sequence of the oligonucleotide, the pattern of guanine oxidation on duplex **2-Rh** was unchanged from the pattern on duplex **1-Rh**. In the absence of protein, oxidation is observed at GG1, GG2, GG3, and GG4, located 8, 11, 16, and 24 bp away from the closest intercalated metal complex. However, there is almost no oxidation at GG5, GG8, GG6, and GG7, located 37, 42, 48, and 56 base pairs from the intercalation site, respectively (Figure 6). As with duplex **1-Rh**, the binding of histone proteins makes very little change in the pattern of oxidation except to very slightly favor oxidation of GG1 and slightly disfavor GG4.

Discussion

Studies with Noncovalently Bound $Rh(phi)_2DMB^{3+}$: Low Accessibility on the Nucleosome Core Particle

Photoexcitation of the rhodium complex in the presence of NCPs promotes the oxidation of the 5′ guanine of 5′-GG-3′ sites with irradiation at both 313 nm and 365 nm. The absence of nonspecific direct strand scission at 313 nm in NCPs indicates that the structure of the core particle clearly diminishes the ability of the noncovalently bound rhodium intercalator to bind to DNA.

Histone proteins are known to protect DNA from binding and cleavage by a variety of small molecules and proteins, such as hydroxyl radical, triple-helix-forming oligonucleotides, DNase I, micrococcal nuclease, and various intercalators [30, 35–44]. In NCPs, histone proteins directly block access to large sections of the major and minor grooves and may electrostatically repel positively charged DNA binding molecules with their own substantial positive charge. Although it has been shown that molecules that bind in the major or minor groove can often bind to nucleosomal DNA wherever their bind-

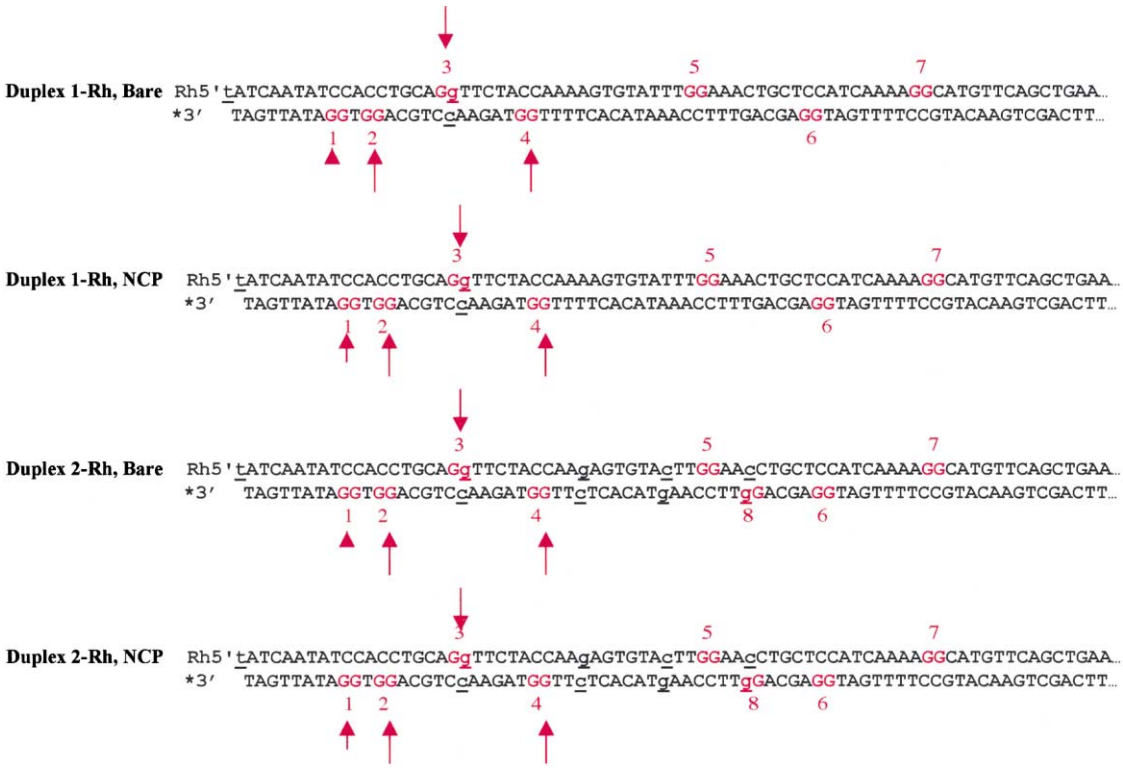

Figure 6. Long-Range Guanine Oxidation by Covalently Tethered Rhodium Complexes

Photoinduced oxidation of 5′-GG-3′ sites (red) by covalently tethered rhodium complexes is indicated by red arrows. The size of the red arrows indicates the extent of oxidation, to a first approximation. Fewer than 1% of strands are oxidized at GG5, GG6, GG7, or GG8.

ing sites are exposed on the solution face of the nucleosome [35, 36, 38, 39], intercalators generally do not bind well to nucleosome core DNA and, where possible, bind instead to linker DNA [40–43]. This exclusion of intercalators from the NCP is thought to occur because the bound histone octamer clamps down on the DNA and prevents the DNA from unstacking and unwinding to accommodate the intercalator.

Like ethidium and other intercalators, the rhodium complex probably intercalates preferentially near the end of the DNA duplex because the DNA near the ends is more floppy and less tightly anchored to the protein than the DNA near the middle of the sequence [24]. The rhodium complex could also intercalate at the middle of the sequence on DNA strands that contain a nick on one strand due to imperfect ligation since related rhodium complexes bind preferentially at base mismatches and other sites of destabilized base stacking [45, 46]. Like other intercalators, the rhodium complex may also bind with lower frequency and affinity at other sites on the NCP that display exposed major grooves and substantial flexibility. Bands due to photoinduced strand scission at 313 nm at intercalation sites near the end, at single-strand nicks, and at low-affinity sites would be difficult to observe on the denaturing acrylamide gel.

Notably, when our noncovalent rhodium intercalator is photoexcited in the presence of the NCP, it selectively promotes the oxidation of all of the 5′ guanines of 5′-GG-3′ sites, *despite* the low accessibility of nucleosomal DNA. The prevalence of this damage on nucleosomal DNA suggests that charges can move through the π stack even when that DNA is bound around a histone octamer. However, these experiments do not establish the distances over which the electronic "hole" can migrate because we do not know with certainty where the rhodium complex is bound.

Studies with Covalently Tethered $Rh(phi)_2bpy^{3+}$: Damage from a Distance

The pattern of guanine base oxidation by $Rh(phi)_2bpy^{3+}$, covalently tethered to the 5′ termini, is almost indistinguishable in the presence and absence of histone proteins. This observation indicates that the wrapping the 146-mer around a histone octamer to form an NCP does not change rhodium intercalation into this sequence nor the long-range charge transport through it (Figure 6). We anticipated a possible difference in the distribution of long-range damage between bare and histone bound DNA due to the mild base stack disruptions caused by the bending of the DNA into a superhelix, the lack of dynamic flexibility in the structure of the DNA when "clamped down" by protein binding, or local structure-dependent effects on charge localization and trapping of the radical species. What is striking is that, despite the multitude of factors that could potentially modulate long-range guanine oxidation, the pattern of oxidation is relatively unchanged by the binding of the DNA to histone proteins as an NCP.

Furthermore, the fact that the pattern of oxidation is

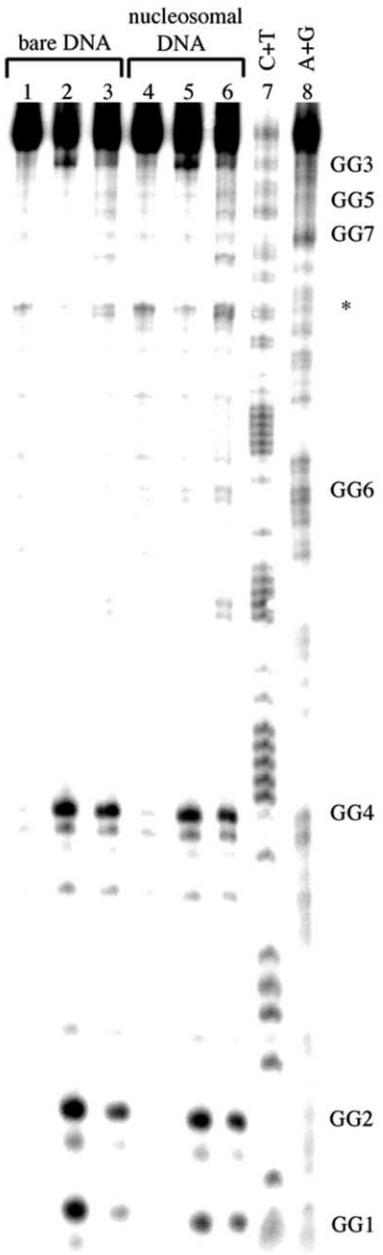

Figure 7. Long-Range Oxidation of 5′-GG-3′ Sites by a Covalently Tethered Rhodium Complex

The oligonucleotide duplex assembly **1-Rh** varies from duplex **1** only in the presence of the covalently tethered metallointercalator at each 5′ end; the sequence of base pairs is the same as that of duplex **1**. The samples shown here contain the left-handed Λ isomer of the rhodium complex; results for the right-handed Δ isomer were the same. Samples shown in lanes 1–3 are bare DNA containing no added histone proteins; lanes 4–6 contain histone proteins bound as a nucleosome core particle. Conditions were as follows: lane 1, no photoirradiation; lane 2, 90 min at 365 nm; lane 3, 15 min at 313 nm; lane 4, no photoirradiation; lane 5, 90 min at 365 nm; and lane 6, 15 min at 313 nm. All samples were treated with hot aqueous piperidine. Lanes 7 and 8 are Maxam-Gilbert pyrimidine-specific and purine-specific sequencing lanes, respectively. Indicated by an asterisk, the band at the center of the gel is due to incomplete ligation to form the 146-mer. 5′-GG-3′ sites are indicated with numbers corresponding to those in Figure 2.

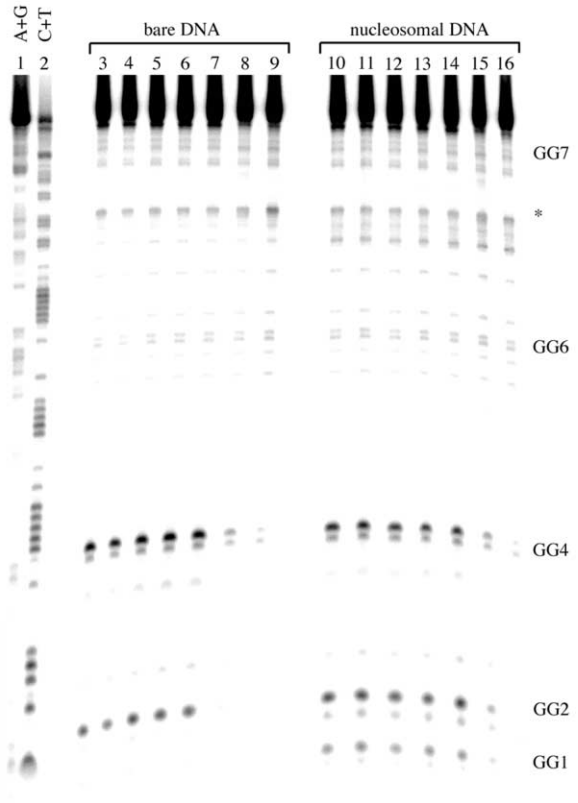

Figure 8. Long-Range Oxidation of 5′-GG-3′ Sites in the Presence and Absence of Bound Histone Proteins at a Range of Temperatures

All samples contain duplex **1-Rh** with the right-handed Δ isomer of the rhodium metallointercalator. Lanes 1 and 2 are Maxam-Gilbert purine-specific and pyrimidine-specific sequencing lanes, respectively. Lanes 3–9 are samples containing bare DNA without histone proteins; samples in lanes 10–16 contain bound histone proteins. All samples were photoirradiated at 365 nm for 1 hr, unless otherwise indicated. Conditions were as follows: lane 3, 5°C; lane 4, 15°C; lane 5, 22°C; lane 6, 27°C; lane 7, 35°C; lane 8, 10 min at 313 nm, 27°C; lane 9, no photoirradiation; lane 10, 5°C; lane 11, 15°C; lane 12, 22°C; lane 13, 27°C; lane 14, 35°C; lane 15, 10 min at 313 nm, 27°C; and lane 16, no photoirradiation. All samples were treated with hot aqueous piperidine. Indicated by an asterisk, the band at the center of the gel is due to incomplete ligation to form the 146-mer. 5′-GG-3′ sites are indicated by numbers corresponding to those in Figure 2.

not changed by binding the DNA to histone proteins as an NCP indicates that the electronic "hole" generated by oxidation of the DNA by rhodium cannot hop from one gyre of the helix to another, despite their close proximity in the core particle (Figure 1B). This inability of the charge to move from one helix to another close by is reminiscent of studies with DNA double-crossover assemblies [47]. There is also no evidence that the rhodium complexes tethered at the 5′ termini can intercalate into neighboring gyres of the DNA.

It is noteworthy that in this 146 bp sequence, no guanine oxidation is observed at guanine doublets GG5, GG6, and GG7, located 38, 48, and 56 bp away from the rhodium intercalator, even in the absence of bound protein. The absence of charge transport to oxidize guanine doublets over this distance contrasts with earlier observations with oligonucleotide duplexes [9, 15]. The

result is, however, perhaps not surprising given that this sequence was designed to favor the bending of DNA so as to form stable NCPs. The oligonucleotide sequence contains a dozen phased nucleosome-positioning sequences, designed to facilitate DNA wrapping around histones as a result of being intrinsically bent in the correct direction for binding to the circular surface of the octamer or by being particularly flexible [24–27]. Such static or dynamic disruptions in base pair stacking would be expected to diminish long-range guanine oxidation [8, 9, 21, 48]. We did not observe oxidation at the more distal 5′-GG-3′ sites in either the presence or absence of histone proteins, even with changes in sequence and temperature designed to improve long-range charge transport. It is quite likely that more systematic and drastic changes in the DNA sequence would increase long-range charge transport to the other 5′-GG-3′ sites in the absence of protein; however, these changes would also probably diminish the affinity of this sequence for the histone octamer and change the structure of the NCP.

Oxidation of Guanine Bases by Charge Transport through the Base Stack in Nucleosomal DNA

In this study we have described the oxidation of guanine doublets in NCPs by rhodium intercalators to determine the effect of DNA packaging on long-range charge transport through the base pair stack. Given that the DNA in the core particle is overwound, bent, and in some places dynamically restricted, it was possible that the binding of DNA to histones in this structure might serve to protect nucleosomal DNA from long-range oxidative damage. Alternatively, such packaging might provide a well-protected, more rigid medium to facilitate charge transport through the DNA base pair stack. The base pair stacking seen in the crystal structure of the NCP is relatively normal (i.e., B form), and the binding of some proteins has previously been shown to increase long-range guanine oxidation by stiffening the helix [21, 22].

The binding of histone proteins to a 146 bp oligonucleotide duplex to form an NCP was observed to radically diminish binding of rhodium complexes to the DNA, consistent with previous research on ethidium and other intercalators. The structure of the NCP is proposed to exclude intercalators by clamping down on the DNA, preventing the unwinding and destacking necessary for intercalation, and thus causing the intercalators to bind preferentially to linker DNA and the termini of core DNA. Notably, despite its radically diminished binding, when our noncovalent rhodium intercalator is photoexcited in the presence of the NCP, it selectively oxidizes all of the 5′ guanines of 5′-GG-3′ sites (Figure 9). This pattern of damage is the signature of charge transport through the DNA base stack, indicating that although the DNA bound as NCPs is relatively protected from attack from small-molecule intercalators by the histone proteins, it is still accessible to damage by long-range oxidation. When the rhodium complex is covalently tethered to the end of the DNA duplex, guanine doublets up to 24 bp away are oxidized through the base stack (Figure 9). This long-range oxidation is not significantly modulated by the binding of the DNA to histone proteins to form

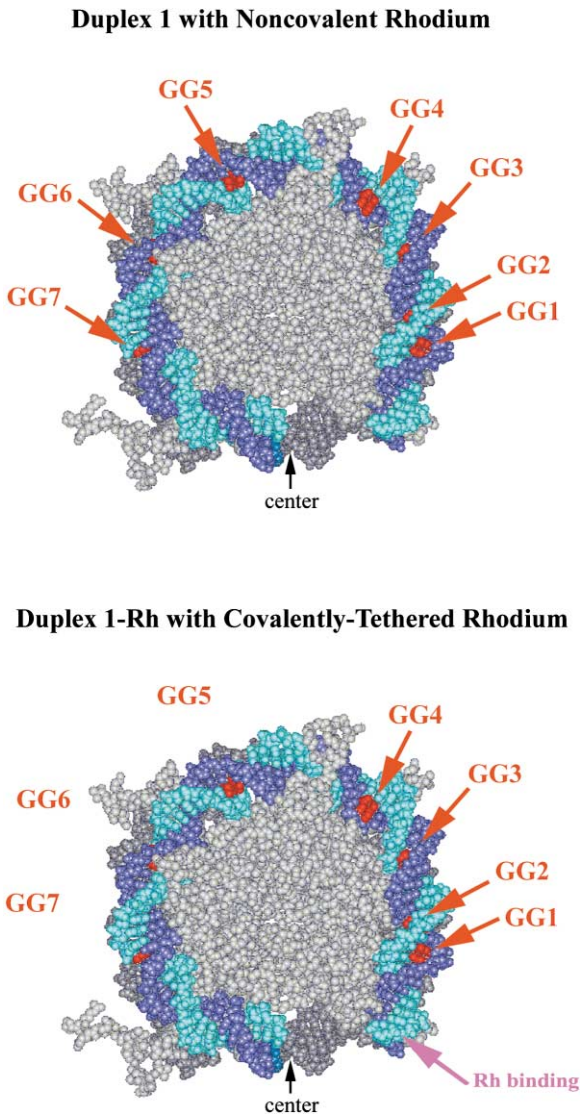

Figure 9. Oxidation of Guanine Doublets in Nucleosomal DNA by Rhodium Metallointercalators

One-half of the palindromic 146 bp sequence is shown in blue and cyan, with 5′-GG-3′ sites highlighted in red and numbered according to Figure 2. The other half of the DNA palindrome, which is identical to this half, and the histone octamer are shown in gray. On the top, although the binding of noncovalent rhodium complexes to duplex **1** is substantially diminished in the presence of histone proteins, these complexes can nonetheless oxidize the 5′ guanine of all seven 5′-GG-3′ sites when photoexcited at 313 or 365 nm (red arrows). This pattern of DNA damage is characteristic of long-range oxidation through the base pair stack. Furthermore, it is clear from this picture that many of the 5′-GG-3′ sites are inaccessible to solution-borne oxidants because the major groove faces inward toward the surface of the histone octamer or is blocked by histone tails. On the right, covalently tethered rhodium complexes intercalate into duplex **1-Rh** near the ends to which they are attached (purple arrow) and oxidize GG1, GG2, GG3, and GG4, corresponding to 5′-GG-3′ sites 8, 11, 16, and 24 bp from the site of intercalation (red arrows). Guanine doublets near the center of the nucleosomal DNA (GG5, GG6, and GG7) were not oxidized either in the presence or absence of protein. The binding of histone proteins to form nucleosomes appears to have very little effect on long-range charge transport through DNA. (The picture was adapted from Protein Data Bank coordinates 1aoi, reference [24].)

an NCP. Clearly, the kinks and flexibility of the DNA sequence alone, which dictates to some large degree its own nucleosomal packaging, have a much larger effect on the ability of charges to move through DNA than does binding to a histone octamer.

Significance

These discoveries have important implications for damage to and repair of the genome in vivo, where much of the DNA is bound within nucleosomal core particles. It has been proposed that histones, in addition to packaging and regulating DNA, also function to protect DNA since the histones reduce binding by a variety of potentially dangerous small molecules. Here we have seen that, in fact, the binding of DNA to histone proteins to form nucleosomal core particles reduces the ability of the rhodium complex to intercalate into the DNA. However, the packaging of DNA as nucleosomes does not protect it from long-range damage through the base pair stack; these photooxidants are still capable of oxidizing guanine bases within the core particle. The long-range oxidation of guanine bases at sites made inaccessible to rhodium complexes by protein binding is consistent also with our observation of the oxidation of guanine doublets and triplets in transcription factor binding sites in the PGK promoter within nuclei [49]. As a consequence, we propose that damage generated on DNA in vivo may be spread from an initial exposed site in "linker" DNA to divergent distal sites within transcriptionally inactive DNA regions that are packaged as nucleosomes. Damage within nucleosomes is likely to be detected and repaired less readily than damage within active and accessible regions of the genome, allowing for the persistence of damaged sites generated by long-range charge transport and the propagation of these damage events to form permanent mutations.

Experimental Procedures

Isolation of Histones

NCPs were isolated from chicken blood as described [25, 30, 50, 51]. Whole chicken blood, collected in sodium citrate, was obtained from Pel Freez Biologicals. After lysis of the cells, nuclei were collected by centrifugation, rinsed profusely, and digested with micrococcal nuclease. After lysis of the nuclei and resuspension of the chromatin, the chromatin was applied to a Sepharose 4B (Sigma) size exclusion column as described. The histone-containing fractions were dialyzed against TE and were evaluated by 18% SDS-polyacrylamide gel electrophoresis and compared to commercially purified histones. These histone fractions were then quantitated via a Coomassie protein assay (Pierce) and used for reconstitution with labeled oligonucleotides. The product that was not needed immediately was stored at −20°C in 50% glycerol with 0.02% sodium azide. These stored fractions were dialyzed against 1× TE (10 mM Tris-HCl, 1 mM EDTA [pH 7.5]) and concentrated with 15 ml Centriprep vials (Amicon) before use.

Preparation of Palindromic 146-mer

DNA sequences used in these experiments were based upon those used by Luger et al. for their structure of the NCP [24, 52] and are shown in Figure 2. Palindromic 146 bp duplexes were made by ligation of identical double-stranded half sequences featuring EcoRI sticky ends.

Single-stranded oligonucleotides were prepared by standard phosphoramidite chemistry and purified by reversed-phase HPLC and preparative denaturing agarose gel electrophoresis [53]. To synthesize duplex **1**, strand "2" was first radiolabeled at its 3′ terminus with α-^{32}P-ddATP (Amersham) and terminal transferase (Boehringer-Mannheim). Samples were precipitated with ethanol, treated with hot aqueous piperidine, and purified on an 8% denaturing agarose gel. After crushing and soaking eluted the DNA from the gel [54], the radiolabeled "2" was purified by Sep-Pak (Waters). Duplex **1** was then prepared by the annealing of equimolar amounts of the complementary strands "1" and "2" (including the radiolabeled strand "2") and ligation of the sticky ends with T4 DNA ligase (New England Biolabs) at 17°C overnight as described previously [9, 53].

For the synthesis of duplex **1-Rh** containing a tethered rhodium complex, a rhodium-tethered 17-mer was ligated to a phosphorylated 59-mer to make a rhodium-tethered 76-mer "3." The 17 bp oligonucleotide with a rhodium complex covalently attached to its 5′ end was prepared and purified as described [55], and a 59 bp oligonucleotide was ligated to its 3′ end to make strand "3." The 76-mer product was purified by denaturing gel electrophoresis as described [9, 53]. The single-stranded, rhodium-tethered oligonucleotide "3" was then desalted by the use of Sep-Pak cartridges and dried in vacuo. Complementary strand "2" was radiolabeled at its 3′ terminus and gel purified as above. Duplex **1-Rh** was then prepared by the annealing of equimolar amounts of strands "3" and "2" (including radiolabeled strand "2") and ligation of the sticky ends with T4 DNA ligase. Duplex **2-Rh** was prepared in a manner identical to the preparation of duplex **1-Rh** with oligonucleotides "4" and "5."

Rhodium complexes were prepared as described previously [56, 57].

Formation of Nucleosome Core Particles with 146-mer

NCPs were formed on the 146-mers by the salt exchange method [29]. To one half of the ligation mixture, histones and salt were added in seven reaction mixtures as follows: 25 μl histone stock solution (approximately 3 mg/ml); 5 μl 10× dilution buffer + β-mercaptoethanol, 12.5 μl 4 M NaCl, and 7.5 μl 146-mer ligation mix in a total volume of 50 μl. The solution was incubated at room temperature for 1 hr. An amount of 16.5 μl 1× dilution buffer (20 mM Tris-HCl [pH 8.0], 1 mM EDTA, and 1 mM β-mercaptoethanol) was added after every hour for 3 hr. Then, 100 μl of 1× dilution buffer was added every 15 min for 1 hr. When the total volume of each reaction reached 500 μl, the solutions were incubated for 1 hr at 37°C. The volume was reduced to <20 μl with Microcon filters (Amicon) and was purified on a 5% nondenaturing acrylamide gel along with the half of the ligation sample to which no protein had been added. The 146-mer and the 146-mer with histones were clearly resolved from each other and from unligated single- and double-stranded 73-mers by electrophoresis for approximately 5 hr at 200 V at ambient temperature. Bands containing the desired samples were excised, and the DNA or DNA-protein complexes were eluted into 1× TE by the crush-and-soak method [54]. The solution was filtered through 0.45 μm filters to remove large pieces of gel and was dialyzed against 1× TE to remove running dye, borate, and acrylamide monomers. After this sample was concentrated with Microcon filters, it was used for DNase I footprints, photoirradiations, or Maxam-Gilbert sequencing reactions. As revealed by both nondenaturing and denaturing gel electrophoresis, this sample contained only histone bound, radiolabeled 146-mer duplexes. A small amount of unlabeled chicken DNA or nucleosomes was probably also present as a carrier in this preparation, but it was of course not visible on the gel and did not interfere with the experiments described here.

DNase I Footprinting of Nucleosomes and Bare DNA and Photoirradiations with $Rh(phi)_2DMB^{3+}$

Samples (30 μl) containing radioactively labeled 146-mer with or without bound histone proteins and 10 μM noncovalently bound rhodium complex (where applicable) were irradiated for up to 2 hr with a 1,000 Hg-Xe arc lamp equipped with a monochromator (Oriel). Samples were maintained around 12°C during irradiation to prevent evaporation. The volume of the stock solution was adjusted to contain a sufficient amount of radioactive label for visualization on the gel after purification and was estimated to contain approximately 50–100 nM 146-mer DNA.

After irradiation, samples were incubated with 50 μg/ml proteinase K in 0.5% SDS for 1.5 hr at 37°C. After digestion, the samples

were treated with 10% piperidine at 90°C for 30 min and dried in vacuo. All samples, including those irradiated at 313 nm, were treated with piperidine to break DNA-protein crosslinks and labilize the DNA at the crosslink site. A DNA fraction directly proportional to the amount of photoirradiation was crosslinked to the histone proteins, and as a result it separated into the organic layer during extraction with phenol, consistent with the results of Nguyen et al. [34]. However, treatment of the photoirradiated, crosslinked DNA with proteinase K and piperidine separated the DNA from the histone protein and broke the DNA strand at the crosslink site. After treatment with proteinase K and piperidine, each sample was resuspended in 100 μl TE, extracted with phenol and chloroform, and precipitated with ethanol before analysis on a 7% denaturing polyacrylamide gel. Gels were quantitated by phosphorimagery with ImageQuant (Molecular Dynamics).

Samples containing radioactively labeled 146-mer with or without bound histone proteins were treated with DNase I [30]. Samples (30 μl) were incubated with varying concentrations of DNase I and 1.25 mM $CaCl_2$ or $MgCl_2$ for 2 min (no histones) or 5 min (with histones) before the reaction was stopped by the addition of 35 μl of stop solution (5.8 M ammonium acetate, 28 mM EDTA, 220 μM bp calf thymus DNA). After thorough mixing, 80 μl of 1% SDS was added. This mixture was extracted with phenol and chloroform and precipitated with ethanol and ammonium acetate before analysis on a 7% denaturing polyacrylamide gel.

Coordinates of the NCP were downloaded from the Protein Data Bank (files 1aoi [24] and 1eqz [28]). Structures were examined with Web Lab Viewer Pro (Accelrys).

Acknowledgments

This work was supported by the National Institutes of Health (GM49216), the National Foundation for Cancer Research, the Howard Hughes Medical Institute predoctoral fellowship program (M.E.N.), and the Caltech SURF program (K.T.N.). We would like to thank Karolin Luger and Armin W. Mäder for advice and protocols regarding the preparation of the palindromic 146-mer.

Received: October 30, 2001
Revised: January 7, 2002
Accepted: January 11, 2002

References

1. Kelley, S.O., and Barton, J.K. (1998). Radical migration through the DNA helix: chemistry at a distance. In Metal Ions in Biological Systems, A. Sigel and H. Sigel, Eds. (New York: Marcel Dekker), pp. 211–249.
2. Núñez, M.E., and Barton, J.K. (2000). Probing DNA charge transport with metallointercalators. Curr. Opin. Chem. Biol. *4*, 199–206.
3. O'Neill, P., and Fielden, E.M. (1993). Primary free radical processes in DNA. Adv. Radiat. Biol. *17*, 53–120.
4. Hall, D.B., Holmlin, R.E., and Barton, J.K. (1996). Oxidative DNA damage through long-range electron transfer. Nature *382*, 731–735.
5. Steenken, S., and Jovanovic, S.V. (1997). How easily oxidizable is DNA? One-electron reduction potentials of adenosine and guanosine radicals in aqueous solution. J. Am. Chem. Soc. *119*, 617–618.
6. Sugiyama, H., and Saito, I. (1996). Theoretical studies of GG-specific photocleavage of DNA via electron transfer: significant lowering of ionization potential and 5′ localization of HOMO of stacked GG bases in B-form DNA. J. Am. Chem. Soc. *118*, 7063–7068.
7. Prat, F., Houk, K.N., and Foote, C.S. (1998). Effect of guanine stacking on the oxidation of 8-oxoguanine in B-DNA. J. Am. Chem. Soc. *120*, 845–846.
8. Hall, D.B., and Barton, J.K. (1997). Sensitivity of DNA-mediated electron transfer to the intervening pi-stack: a probe for the integrity of the DNA base stack. J. Am. Chem. Soc. *119*, 5045–5046.
9. Núñez, M.E., Hall, D.B., and Barton, J.K. (1999). Long-range oxidative damage to DNA: effects of distance and sequence. Chem. Biol. *6*, 85–97.
10. Arkin, M.R., Stemp, E.D.A., Coates Pulver, S., and Barton, J.K. (1997). Long-range oxidation of guanine by Ru(III) in duplex DNA. Chem. Biol. *4*, 389–400.
11. Stemp, E.D.A., Arkin, M.R., and Barton, J.K. (1997). Oxidation of guanine in DNA by $Ru(phen)_2dppz^{3+}$ using the flash-quench technique. J. Am. Chem. Soc. *119*, 2921–2925.
12. Hall, D.B., Kelley, S.O., and Barton, J.K. (1998). Long-range and short-range oxidative damage to DNA: photoinduced damage to guanines in ethidium-DNA assemblies. Biochemistry *37*, 15933–15940.
13. Henderson, P.T., Jones, D., Hampikian, G., Kan, Y., and Schuster, G. (1999). Long-distance charge transport in duplex DNA: the phonon-assisted polaron-like hopping model. Proc. Natl. Acad. Sci. USA *96*, 8353–8358.
14. Gasper, S.M., and Schuster, G.B. (1997). Intramolecular photoinduced electron transfer to anthraquinones linked to duplex DNA: the effect of gaps and traps on long-range radical cation migration. J. Am. Chem. Soc. *119*, 12762–12771.
15. Schuster, G.B. (2000). Long-range charge transfer in DNA: transient structural distortions control the distance dependence. Acc. Chem. Res. *33*, 253–260.
16. Bixon, M., Giese, B., Wessely, B., Langenbacher, T., Michel-Beyerle, M.E., and Jortner, J. (1999). Long-range charge hopping in DNA. Proc. Natl. Acad. Sci. USA *96*, 11713–11716.
17. Giese, B. (2000). Long-distance charge transport in DNA: the hopping mechanism. Acc. Chem. Res. *33*, 631–636.
18. Núñez, M.E., Noyes, K.T., Gianolio, D.A., McLaughlin, L.W., and Barton, J.K. (2000). Long-range guanine oxidation in DNA restriction fragments by a triplex-directed naphthalene diimide intercalator. Biochemistry *39*, 6190–6199.
19. Nakatani, K., Dohno, C., and Saito, I. (2000). Modulation of DNA-mediated hole-transport efficiency by changing superexchange electronic interaction. J. Am. Chem. Soc. *122*, 5893–5894.
20. Lewin, B. (2000). Genes VII. (Oxford, UK: Oxford University Press).
21. Rajski, S.R., Kumar, S., Roberts, R.J., and Barton, J.K. (1999). Protein-modulated DNA electron transfer. J. Am. Chem. Soc. *121*, 5615–5616.
22. Rajski, S.R., and Barton, J.K. (2001). How different DNA-binding proteins affect long-range oxidative damage to DNA. Biochemistry *40*, 5556–5564.
23. Kornberg, R.D., and Lorch, Y. (1999). Twenty-five years of the nucleosome, fundamental particle of the eukaryote chromosome. Cell *98*, 285–294.
24. Luger, K., Mäder, A., Richmond, R., Sargent, D., and Richmond, T.J. (1997). Crystal structure of the nucleosome core particle at 2.8 Å resolution. Nature *389*, 251–260.
25. Drew, H., and Calladine, C. (1987). Sequence-specific positioning of core histones on an 860 base-pair DNA. J. Mol. Biol. *195*, 143–173.
26. Fitzgerald, D.J., and Anderson, J.N. (1998). Unique translational positioning of nucleosomes on synthetic DNAs. Nucleic Acids Res. *26*, 2526–2535.
27. Shrader, T.E., and Crothers, D.M. (1989). Artificial nucleosome positioning sequences. Proc. Natl. Acad. Sci. USA *86*, 7418–7422.
28. Harp, J.M., Hanson, B.L., Timm, D.E., and Bunick, G.J. (2000). Asymmetries in the nucleosome core particle at 2.5 Å resolution. Acta Crystallogr. D *56*, 1513–1534.
29. Hayes, J.J., and Lee, K.-M. (1997). *In vitro* reconstitution and analysis of mononucleosomes containing defined DNAs and proteins. Methods *12*, 2–9.
30. Lutter, L. (1989). Digestion of nucleosomes with deoxyribonucleases I and II. Methods Enzymol. *170*, 264–269.
31. Sitlani, A., Long, E.C., Pyle, A.M., and Barton, J.K. (1992). DNA photocleavage by phenanthrenequinone diimine complexes of rhodium(III): shape-selective recognition and reaction. J. Am. Chem. Soc. *114*, 2302–2312.
32. Uchida, K., Pyle, A.M., Morii, T., and Barton, J.K. (1989). High-resolution footprinting of EcoRI and distamycin with $Rh(phi)_2(bpy)^{3+}$, a new photofootprinting reagent. Nucleic Acids Res. *17*, 10259–10279.

33. Burrows, C.J., and Muller, J.G. (1998). Oxidative nucleobase modifications leading to strand scission. Chem. Rev. *98*, 1109–1159.
34. Nguyen, K.L., Steryo, M., Kurbanyan, K., Nowitzki, K., Butterfield, S., Ward, S., and Stemp, E.D.A. (2000). DNA-protein cross-linking from oxidation of guanine via the flash-quench technique. J. Am. Chem. Soc. *122*, 3585–3594.
35. Bellard, M., Dretzen, G., Giangrande, A., and Ramain, P. (1989). Nuclease digestion of transcriptionally active chromatin. Methods Enzymol. *170*, 317–346.
36. Cartwright, I., and Elgin, C. (1989). Nonenzymatic cleavage of chromatin. Methods Enzymol. *170*, 359–369.
37. Brown, P., and Fox, K. (1996). Nucleosome core particles inhibit DNA triplex helix formation. Biochem. J. *319*, 607–611.
38. Gottesfeld, J.M., Melander, C., Suto, R.K., Raviol, H., Luger, K., and Dervan, P. (2001). Sequence-dependent recognition of DNA in the nucleosome by pyrrole-imidazole polyamides. J. Mol. Biol. *309*, 615–629.
39. Millard, J.T. (1996). DNA modifying agents as tools for studying chromatin structure. Biochimie *78*, 803–816.
40. McMurray, C.T., and van Holde, K.E. (1991). Binding of ethidium to the nucleosome core particle. 1. Binding and dissociation reactions. Biochemistry *30*, 5631–5643.
41. McMurray, C.T., Small, E.W., and van Holde, K.E. (1991). Binding of ethidium to the nucleosome core particle. 2. Internal and external binding modes. Biochemistry *20*, 5644–5652.
42. Chaires, J.B., Dattagupta, N., and Crothers, D.M. (1983). Binding of daunomycin to calf thymus nucleosomes. Biochemistry *22*, 284–292.
43. Hagmar, P., Pierrou, S., Nielsen, P., Nordén, B., and Kubista, M. (1992). Ionic strength dependence of the binding of methylene blue to chromatin and calf thymus DNA. J. Biomol. Struct. Dyn. *9*, 667–679.
44. Yu, L., Goldberg, I., and Dedon, P. (1994). Enediyne-mediated DNA damage in nuclei is modulated at the level of the nucleosome. J. Biol. Chem. *269*, 4144–4151.
45. Jackson, B.A., and Barton, J.K. (1997). Recognition of DNA base mismatches by a rhodium intercalator. J. Am. Chem. Soc. *119*, 12986–12987.
46. Jackson, B.A., Alekseyev, V.Y., and Barton, J.K. (1999). A versatile mismatch recognition agent: specific cleavage of a plasmid DNA at a single base mispair. Biochemistry *38*, 4655–4662.
47. Odom, D.T., Dill, E.A., and Barton, J.K. (2000). Robust charge transport in DNA double crossover assemblies. Chem. Biol. *7*, 475–481.
48. Williams, T.T., Odom, D.T., and Barton, J.K. (2000). Variations in DNA charge transport with nucleotide composition and sequence. J. Am. Chem. Soc. *122*, 9048–9049.
49. Núñez, M.E., Holmquist, G.H., and Barton, J.K. (2001). Evidence for DNA charge transport in the nucleus. Biochemistry *40*, 12465–12471.
50. Lutter, L. (1978). Kinetic analysis of deoxyribonuclease I cleavages in the nuclesome core: evidence for a DNA superhelix. J. Mol. Biol. *124*, 391–420.
51. Kornberg, R.D., LaPointe, J.W., and Lorch, Y. (1978). Preparations of nucleosomes and chromatin. Methods Enzymol. *170*, 3–14.
52. Luger, K., Rechsteiner, T.J., and Richmond, T.J. (1999). Preparation of nucleosome core particles from recombinant histones. Methods Enzymol. *304*, 3–19.
53. Núñez, M.E., Rajski, S.R., and Barton, J.K. (2000). Damage to DNA by long-range charge transport. Methods Enzymol. *319*, 165–188.
54. Sambrook, J., Fritsch, E.F., and Maniatis, T. (1989). Molecular Cloning: A Laboratory Manual, Second Edition. (Cold Spring Harbor, NY: Cold Spring Harbor Laboratory Press).
55. Holmlin, R.E., Dandliker, P.J., and Barton, J.K. (1999). Synthesis of metallointercalator-DNA conjugates on a solid support. Bioconj. Chem. *10*, 1122–1130.
56. Pyle, A.M., Chiang, M.Y., and Barton, J.K. (1990). Synthesis and characterization of physical, electronic, and photochemical aspects of 9,10 phenanthenequinone diimine complexes of ruthenium(II) and rhodium(III). Inorg. Chem. *29*, 4487–4495.
57. Sitlani, A., and Barton, J.K. (1994). Sequence-specific recognition by phenanthrenequinone diimine complexes of rhodium(III): importance of steric and van der Waals interactions. Biochemistry *33*, 12100–12108.
58. Kielkopf, C.L., Erkkila, K.E., Hudson, B.P., Barton, J.K., and Rees, D.C. (2000). Structure of a photoactive rhodium complex intercalated into DNA. Nat. Struct. Biol. *7*, 117–121.